nature physics

LETTERS

PUBLISHED ONLINE: 22 MARCH 2009 | DOI: 10.1038/NPHYS1221

# Polychromatic dynamic localization in curved photonic lattices

Alexander Szameit[1]*, Ivan L. Garanovich[2], Matthias Heinrich[1], Andrey A. Sukhorukov[2], Felix Dreisow[1], Thomas Pertsch[1], Stefan Nolte[1], Andreas Tünnermann[1] and Yuri S. Kivshar[2]

**Dynamic localization is the suppression of the broadening of a charged-particle wave packet as it moves along a periodic potential in an a.c. electric field[1–3]. The same effect occurs for optical beams in curved photonic lattices, where the lattice bending has the role of the driving field, and leads to the cancellation of diffraction[4–8]. Dynamic localization was also observed for Bose–Einstein condensates[9], and could have a role in the spin dynamics of molecular magnets[10]. It has been predicated that dynamic localization will occur in multi-dimensional lattices at a series of resonances between lattice, particle and driving-field parameters[1]. However, only the first dynamic localization resonance in one-dimensional lattices has been observed in any physical system[6–9]. Here, we report on the experimental observation of higher-order and mixed dynamic localization resonances in both one- and two-dimensional photonic lattices. New features such as spectral broadening of the dynamic localization resonances and localization-induced transformation of the lattice symmetry are demonstrated. These phenomena could be used to shape polychromatic beams emitted by supercontinuum light sources[11,12].**

In optics, the effect of an external electric field on the motion of charged particles in periodic potentials can be mimicked by the propagation of a laser beam in an array of curved waveguides[13]. A schematic diagram of a one-dimensional waveguide array is shown in Fig. 1a. In such a structure, light propagation is governed by coupling between the modes of neighbouring waveguides, similar to wave dynamics in discrete lattices[14]. Constant waveguide curvature corresponds to a d.c. field, and in this case the beam experiences Bloch oscillations[13], which have also been observed in straight optical lattices with transversely modulated parameters[15–18]. Dynamic localization due to a.c. fields can then be observed in arrays of periodically curved optical waveguides with alternating curvature[5,6,8]. A zigzag bending leads to similar behaviour[4], and arrays with optimized discontinuous waveguide curvature also enable us to compensate for the long-range coupling between the non-nearest waveguide modes[7]. In straight waveguide arrays, optical beams experience broadening due to discrete diffraction[14], whereas in the regime of Bloch oscillations or dynamic localization a periodic reconstruction of the initial light distribution occurs. Whereas the effective d.c. driving field always leads to Bloch oscillations with a period proportional to the inverse driving amplitude, dynamic localization is a resonant effect that occurs only for certain relations between the a.c. field profiles and the wave-particle parameters. By adjusting the detuning from the dynamic localization resonance, it becomes possible to control the rate of wave transport. For light propagating in curved waveguide arrays, the detuning depends on the wavelength, and application

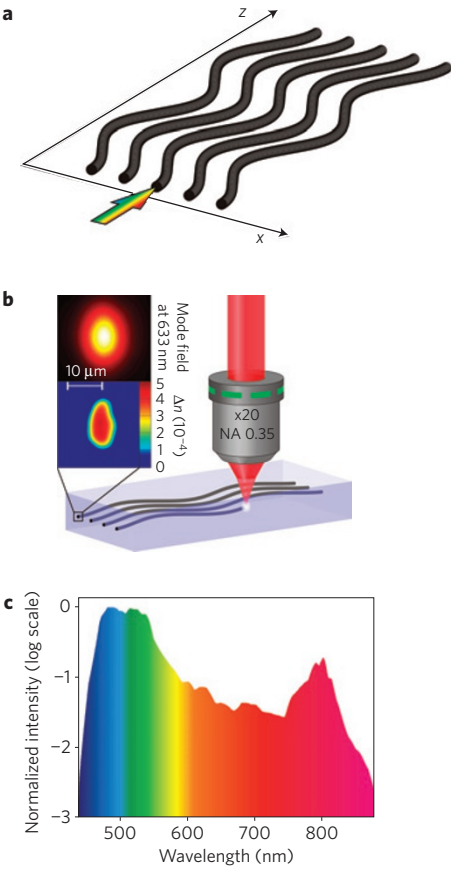


**Figure 1 | Polychromatic light in modulated photonic lattices.** **a**, Schematic diagram of a one-dimensional periodically curved waveguide array, in which a white-light supercontinuum is launched. **b**, Schematic diagram of the femtosecond writing procedure. Insets: The resulting waveguide refractive index modulation $\Delta n$ (bottom) and mode (top) profiles. **c**, The broadband supercontinuum spectrum spanning the entire visible region.

of this effect for optical filtering has been suggested[19]. By exploring the shaping of polychromatic light, we identify and characterize different dynamic localization resonances in lattices of various geometries and dimensionalities.

For our experiments, we use the laser direct-writing method in fused-silica glass (see the schematic diagram of the writing set-up in Fig. 1b) to fabricate one- and two-dimensional

[1]Institute of Applied Physics, Friedrich-Schiller-University Jena, Max-Wien-Platz 1, 07743 Jena, Germany, [2]Nonlinear Physics Centre, Research School of Physics and Engineering, Australian National University, Canberra, ACT 0200, Australia. *e-mail: alexander.szameit@uni-jena.de.

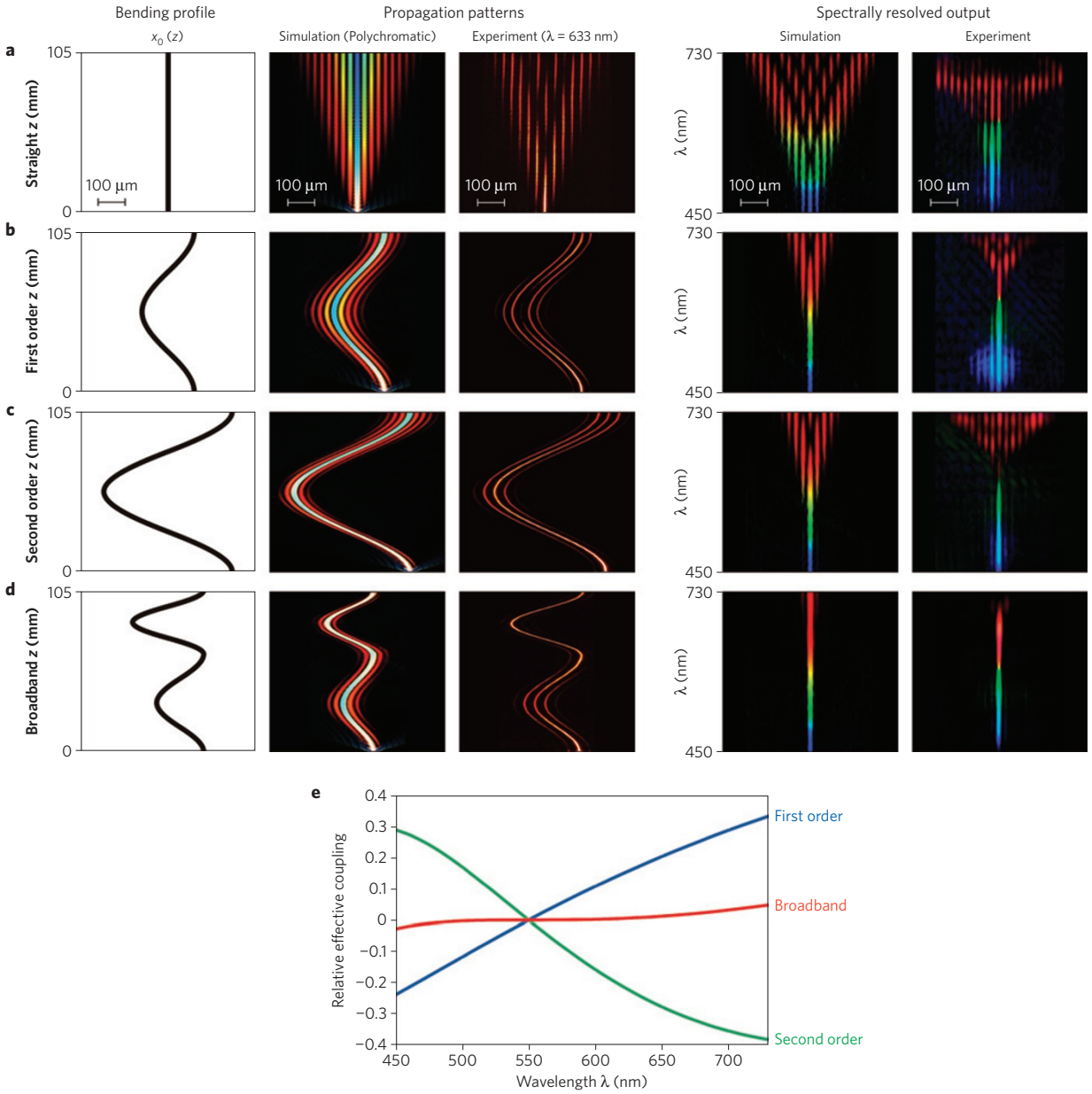


**Figure 2 | Dynamic localization of white light. a**, Diffraction in a straight waveguide array. **b**, First-order dynamic localization at the wavelength $\lambda = 550$ nm. **c**, Second-order dynamic localization at the wavelength $\lambda = 550$ nm. **d**, Broadband dynamic localization in the spectral region 450–730 nm in a two-segment curved array. First column: waveguide axes bending profiles. Second and third columns: numerical simulations of the polychromatic beam propagation and corresponding fluorescent images measured at the wavelength $\lambda = 633$ nm. Fourth and fifth columns: numerically calculated and experimentally measured spectrally resolved output beam profiles. **e**, Effective couplings in the curved arrays shown in **b**–**d** as a function of the wavelength.

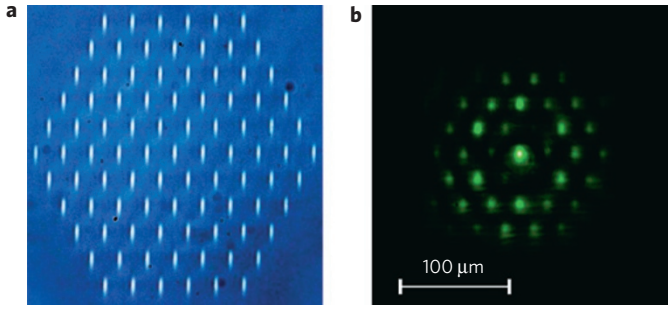


**Figure 3 | Hexagonal lattice. a**, Microscope image of the fabricated hexagonal lattice. **b**, Output diffraction pattern observed in the straight hexagonal array at $\lambda = 543$ nm.

waveguide arrays with required bending profiles. To characterize comprehensively light propagation in the fabricated arrays, we use two complementary methods: (1) direct visualization of the laser beam propagation at $\lambda = 633$ nm through fluorescence imaging, and (2) spectrally resolved imaging of the output optical field distribution for the broadband supercontinuum excitation that spans over the entire visible ($\lambda = 450$–$800$ nm) (see Fig. 1c). First, we measure beam evolution in straight waveguide arrays (see Fig. 2a). The beam propagation calculated theoretically for the supercontinuum light and registered experimentally for the wavelength $\lambda = 633$ nm is shown in the second and third columns, respectively. In the fourth and fifth columns, we present the calculated and measured spectrally resolved output beam profiles, respectively. Note that diffraction increases at longer wavelengths, in agreement with previous studies[20,21].

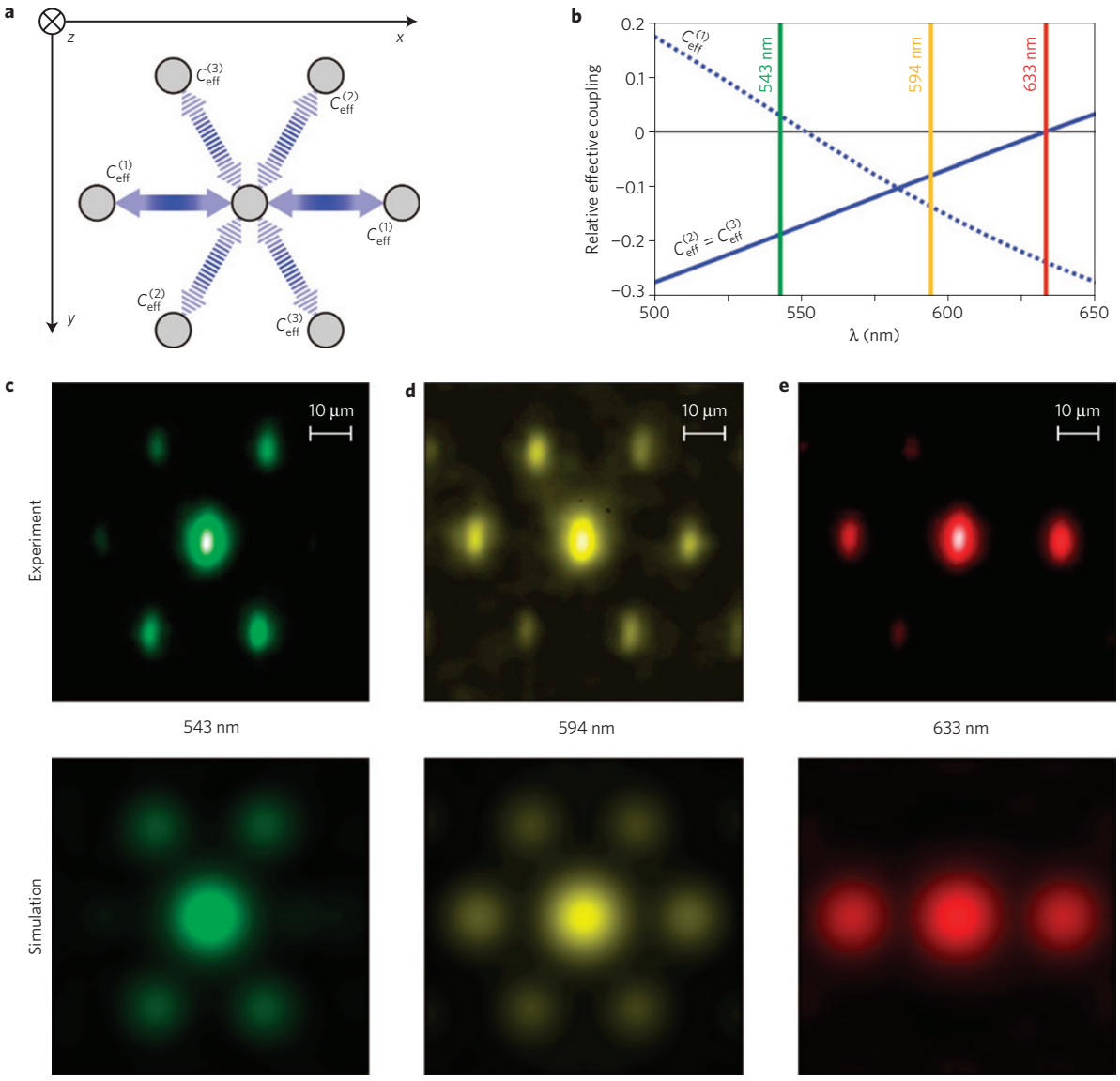


**Figure 4 | Spatial–spectral beam shaping in a two-dimensional lattice. a**, Schematic diagram of the effective couplings in the modulated hexagonal lattice. **b**, Wavelength dependence of the effective couplings. **c**–**e**, Output diffraction profiles of light beams measured experimentally (top) and calculated numerically (bottom) in the same modulated hexagonal lattice at three different wavelengths: 543 nm (**c**), 594 nm (**d**) and 633 nm (**e**).

To provide a link with the classical dynamic localization effect in one-dimensional lattices, we consider planar arrays with harmonic waveguide bending profiles. Then, after each bending period the beam diffraction in the periodically curved waveguide array is characterized by the effective coupling coefficient between the neighbouring waveguides $C_{\mathrm{eff}} = C(\lambda)J_0(\xi/\lambda)$, where $\lambda$ is the optical wavelength, $C(\lambda)$ is the coupling coefficient between straight waveguides, $J_0$ is the Bessel function and $\xi$ is a parameter that depends only on the lattice geometry. Dynamic localization occurs when the effective coupling is reduced to zero, which happens at a series of resonances between the wavelength of light and the lattice parameters: $\xi/\lambda = \rho_n$, where $\rho_n$ are the roots of the Bessel function[6] (see the Methods section for details). Accordingly, for a given structure, dynamic localization is possible only for specific colours of light. The first-order dynamic localization was previously observed experimentally[6], yet higher-order resonances were not explored. Below, we demonstrate that by accessing higher-order dynamic localization and introducing mixed resonances, it becomes possible to realize a new regime of dynamic localization with strongly broadened response.

We create two sets of waveguide arrays with the same parameters except for different bending amplitudes, which are chosen to satisfy the first- and second-order dynamic localization resonance condition at the wavelength of $\lambda_0 = 550$ nm. The corresponding results are presented in Fig. 2b and c, respectively. We observe that, in both structures, the frequency components in a narrow spectral region around $\lambda_0$ return to a single waveguide at the output, whereas significant diffractive broadening occurs for other wavelengths. This is in sharp contrast to the light propagation in the same straight waveguide array without bending, where all spectral components experience strong diffraction (see Fig. 2a). To understand the difference between the dynamic localization of different orders, we present in Fig. 2e wavelength dependencies of the corresponding effective coupling coefficients. For the first-order dynamic localization, $C_{\mathrm{eff}}$ changes sign from negative to positive at the resonance when we move from shorter to longer wavelengths, corresponding to the transition from anomalous to normal discrete diffraction. In contrast, the sign changes from positive to negative around the second-order dynamic localization resonance.

The difference between dynamic localization of different orders for polychromatic light suggests that multi-colour beams can be manipulated through a combination of several dynamic localization resonances[22]. Specifically, we find that it is possible to achieve approximate dynamic localization in an extremely broad spectral region by combining two successive segments of the curved waveguide array that are tuned to the first- and second-order dynamic localization at the same wavelength (see the corresponding waveguide bending profile in Fig. 2d).

Then, although different colours detuned from the exact dynamic localization wavelength exhibit non-zero diffraction after the propagation in the first segment, the input beam profile is restored through the reversed diffraction in the second segment. The overall effective coupling in the two-segment structure almost completely vanishes in a very broad spectral region around the dynamic localization resonance wavelength (Fig. 2e, red line). In Fig. 2d, light propagation and output beam profiles are shown for the two-segment curved waveguide array. We observe that all spectral components, from $\lambda = 450$ to 730 nm, are localized in a single waveguide at the array output (Fig. 2d, fourth and fifth columns), despite the highly non-trivial evolution of different spectral components inside the structure (Fig. 2d, second and third columns).

Next, we explore new features of the dynamic localization effect that arise in higher dimensions. Although dynamic localization was predicted for three-dimensional electronic systems[1], only one-dimensional dynamic localization has been observed experimentally so far[6,7]. Using the laser direct-writing technique, we can create arbitrary two-dimensional lattices. As an example, we consider a hexagonal lattice (see the microscope image of the fabricated structure in Fig. 3a). In a straight lattice, the diffraction pattern has the six-fold symmetry according to the underlying lattice, see Fig. 3b. To compare the results with one-dimensional lattices, we consider the simple harmonic bending profile in the $x$–$z$ plane: $x_0(z) = A\cos[2\pi z/L]$, where $A$ and $L$ are the bending amplitude and period, respectively, and $x_0(z)$ is the lattice transverse shift along the $x$ axis. Although the waveguides are modulated in one plane, this affects coupling between the neighbouring waveguides along different directions, defined by the coefficients $C_{\rm eff}^{(1)}$, $C_{\rm eff}^{(2)}$ and $C_{\rm eff}^{(3)}$ as shown in Fig. 4a. The effective coupling coefficients can be expressed as follows[23]: $C_{\rm eff}^{(1)} = C(\lambda)J_0(\xi/\lambda)$, $C_{\rm eff}^{(2)} = C_{\rm eff}^{(3)} = C(\lambda)J_0(\xi/2\lambda)$, and their wavelength dependencies for the fabricated array are presented in Fig. 4b. We see that the horizontal and diagonal coupling coefficients may vanish at different wavelengths, corresponding to partial dynamic localization along particular lattice directions. In the fabricated hexagonal lattice, the diagonal couplings are suppressed at the wavelength $\lambda = 633$ nm (see the red line in Fig. 4b). In this spectral region, light effectively experiences one-dimensional diffraction, see Fig. 4e. On the other hand, for $\lambda = 583$ nm, all three couplings are reduced simultaneously by the same factor $-0.1$, and the diffraction symmetry of the original hexagonal lattice is preserved. Output diffraction profiles at the closely tuned wavelength $\lambda = 594$ nm are shown in Fig. 4d, where a pronounced hexagonal diffraction pattern is visible (corresponding effective couplings are marked with the yellow line in Fig. 4b). Finally, at $\lambda = 550$ nm the horizontal coupling is cancelled ($C_{\rm eff}^{(1)} = 0$). At this wavelength, the beam can still spread across the whole lattice, yet the diffraction pattern is similar to those of square or rectangular lattices where each lattice site is coupled to its four immediate neighbours (see Fig. 4c). Effective couplings at the wavelength $\lambda = 543$ nm are marked with the green line in Fig. 4b.

Our results demonstrate novel fundamental features of the effect of dynamic localization based on higher-order and mixed resonances in one- and two-dimensional lattices. Polychromatic dynamic localization and localization-induced transformation of lattice geometry, which we observe for the first time to our knowledge, open up new avenues for applications of the dynamic localization effect in various physical contexts. In particular, our work suggests new approaches for flexible shaping of polychromatic light with ultrabroadband or supercontinuum spectra[11,12], which can be enhanced further through the introduction of structure tunability and optical nonlinearities.

## Methods

**Theory of dynamic localization in curved waveguides.** To understand the origins of the dynamic localization effect, we note that light propagation in an array of weakly coupled waveguides can be considered as effectively discretized[14], and it is primarily characterized by coupling due to the overlap between the fundamental modes of the nearest-neighbouring waveguides. Second-order coupling between non-nearest neighbours is weak under our experimental conditions and is not taken into account. In a one-dimensional array, light propagation can be described by a set of equations for the mode amplitudes $\psi_m(z)$ (ref. 6), $i{\rm d}\psi_m/{\rm d}z + C(\lambda)[\psi_{m+1} + \psi_{m-1}] = (2\pi n_0 d/\lambda)\ddot{x}_0(z)m\psi_m$. Here, $z$ is the propagation distance along the waveguides, $m$ is the waveguide number, the coefficient $C(\lambda)$ defines the coupling strength between the neighbouring waveguides that depends on the wavelength $\lambda$, $n_0$ is the refractive index of the medium, $d$ is the waveguide spacing, the function $x_0(z)$ describes periodic waveguide bending in a curved array and dots stand for the derivatives. By the substitution $z \to t$, the spatial light evolution in a curved optical waveguide array becomes fully analogous to the temporal evolution of a quantum particle in an externally driven periodic potential, where $\psi_m(t)$ have the role of the probability amplitudes, $C(\lambda)$ is replaced by the nearest-neighbour transfer-matrix element and the driving force $x_0(t)$ is determined by the external electric field[1].

In a straight waveguide array (with $x_0(z) \equiv 0$), the dispersion relation reads $k_z = 2C(\lambda)\cos(k_x d)$, where $k_z$ and $k_x$ are longitudinal and transverse components of the wave vector, respectively[4]. Accordingly, the diffraction strength for a broad beam is determined as $D = \partial^2 k_z/\partial k_x^2 = -2C(\lambda)d^2\cos(k_x d)$ (ref. 4). In a periodically curved array, wave diffraction after each bending period ($z \to z + L$) can be described by a similar relation where $C(\lambda)$ is replaced by the effective coupling, which is a functional of a specific bending profile[6], $C_{\rm eff} = C(\lambda)L^{-1}\int_0^L \cos[2\pi n_0 {\rm d}\dot{x}_0(\zeta)/\lambda]{\rm d}\zeta$. For a harmonic bending profile $x_0(z) = A\cos[2\pi z/L]$ with bending amplitude $A$, the effective coupling reads $C_{\rm eff} = C(\lambda)J_0(\xi/\lambda)$, where $\xi = 4\pi^2 n_0 dA/L$. Thus, when $\xi/\lambda = \rho_n$, where $\rho_n \simeq 2.40, 5.52, \ldots$ is the $n$ th root of the Bessel function $J_0$, the effective coupling vanishes, $C_{\rm eff} = 0$. This regime corresponds to the periodic diffraction cancellation, $D_{\rm eff} = -2C_{\rm eff}d^2\cos(k_x d) = 0$, which is called dynamic localization[1,6]. Note that the dynamic localization resonances do not depend on the dispersion of the coupling coefficient $C(\lambda)$. The effective coupling method can also be generalized to higher dimensions[1,23].

In our numerical simulations, we use a continuous $(1+1)$- and $(2+1)$-dimensional finite-difference beam propagation method to model light propagation in one- and two-dimensional waveguide arrays, respectively[22,23] (the numbers in brackets denote the number of transverse and longitudinal spatial dimensions, respectively). For polychromatic beams, we use a superposition of 50 frequency components with an equidistant flat spectrum from 450 to 730 nm as input. Slight differences between the theoretical and experimental results appear for the one-dimensional arrays because in numerical modelling we do not account for the two-dimensional mode reshaping. Nevertheless, this has no effect on the position of dynamic localization resonances, as they do not depend on the mode overlaps as detailed above.

**Laser writing.** Our samples are fabricated in fused silica using the femtosecond laser direct-writing technique[24]. When ultrashort laser pulses are tightly focused into a transparent bulk material, nonlinear absorption takes place leading to optical breakdown and the formation of a microplasma, which induces a permanent change in the molecular structure of the material. In the case of silica glass, the density is locally increased. By moving the sample transversely with respect to the beam, a continuous modification of the refractive index is obtained enabling light guiding (see the schematic diagram in Fig. 1b). This technique can be used to create large waveguiding structures with almost arbitrary three-dimensional topology[25]. Details of the fabrication technique can be found elsewhere[26]. All of our samples are 105 mm long with the waveguide spacing $d = 26\,\mu$m. Laser-written waveguides possess an elliptical transverse cross-section of approximately $4 \times 13\,\mu{\rm m}^2$. The profiles of the waveguide refractive index distribution and the corresponding mode measured at $\lambda = 633$ nm are shown as insets in Fig. 1b. To study one-dimensional dynamic localization, we created three curved waveguide arrays consisting of 19 waveguides each. Curved arrays for the first- and second-order dynamic localization contain one full bending period equal to the sample length ($L = 105$ mm), and have bending amplitudes $A = 93$ and $214\,\mu$m, respectively. The curved array for the broadband dynamic localization consists of two successive segments of length $L_1 = 63$ mm and $L_2 = 42$ mm with bending amplitudes $A_1 = 56\,\mu$m and $A_2 = 86\,\mu$m, respectively. To study dynamic localization in two-dimensional

lattices, we created a curved hexagonal array with a bending period $L = 105$ mm and bending amplitude $A = 215$ μm (see the microscope image of the fabricated array in Fig. 3a). To characterize the diffraction strength in our samples, we also fabricated one- and two-dimensional straight arrays (see the measured diffraction patterns in the straight arrays in Figs 2a and 3b).

**Fluorescence imaging.** To directly observe the light propagation within our one-dimensional arrays (see Fig. 2, third column), we use a fluorescence technique[27]. For the fabrication of the waveguides, we use fused silica with a high content of hydroxide. This leads to a massive formation of non-bridging oxygen hole centres during the writing process, resulting in a homogeneous spatial distribution of these colour centres along the waveguides. When launching light from a HeNe laser at $\lambda = 633$ nm into the waveguides, the non-bridging oxygen hole centres are excited and the resulting fluorescence ($\lambda = 650$ nm) can be directly observed[8]. As the colour centres are formed exclusively inside the waveguides, this technique yields a high signal-to-noise ratio. In contrast to fluorescent polymers (see, for example, ref. 28), the bulk material causes almost no background noise in our case.

**Supercontinuum characterization.** A white-light continuum was generated using a 25-cm-long photonic-crystal fibre (PCF NL-1.7-650, Crystal Fibre). Ultrashort laser pulses with a length of 1 ps from a Ti:sapphire oscillator (Spectra Physics) were coupled into the photonic-crystal fibre. Owing to the high peak power of these pulses, supercontinuum radiation was generated with a spectrum shown in Fig. 1c. This white light is coupled into the central waveguide of the arrays using a ×10 microscope objective (numerical aperture: 0.25). The output facet is imaged onto a CCD (charge-coupled device) camera by a ×10 microscope objective; the spectral resolution is achieved by a prism placed between the objective and the camera. Owing to the chromatic dispersion, the output spatial profiles are resolved at the individual wavelengths[29,30] (see Fig. 2, fifth column).

Received 15 October 2008; accepted 11 February 2009; published online 22 March 2009

## References


1. Dunlap, D. H. & Kenkre, V. M. Dynamic localization of a charged particle moving under the influence of an electric field. *Phys. Rev. B* **34**, 3625–3633 (1986).
2. Holthaus, M. Collapse of minibands in far-infrared irradiated superlattices. *Phys. Rev. Lett.* **69**, 351–354 (1992).
3. Dignam, M. M. & de Sterke, C. M. Conditions for dynamic localization in generalized ac electric fields. *Phys. Rev. Lett.* **88**, 046806 (2002).
4. Eisenberg, H. S., Silberberg, Y., Morandotti, R. & Aitchison, J. S. Diffraction management. *Phys. Rev. Lett.* **85**, 1863–1866 (2000).
5. Lenz, G., Parker, R., Wanke, M. C. & de Sterke, C. M. Dynamical localization and AC Bloch oscillations in periodic optical waveguide arrays. *Opt. Commun.* **218**, 87–92 (2003).
6. Longhi, S. *et al.* Observation of dynamic localization in periodically curved waveguide arrays. *Phys. Rev. Lett.* **96**, 243901 (2006).
7. Iyer, R., Aitchison, J. S., Wan, J., Dignam, M. M. & de Sterke, C. M. Exact dynamic localization in curved AlGaAs optical waveguide arrays. *Opt. Express* **15**, 3212–3223 (2007).
8. Dreisow, F. *et al.* Spectral resolved dynamic localization in curved fs laser written waveguide arrays. *Opt. Express* **16**, 3474–3483 (2008).
9. Madison, K. W., Fischer, M. C., Diener, R. B., Niu, Q. & Raizen, M. G. Dynamical Bloch band suppression in an optical lattice. *Phys. Rev. Lett.* **81**, 5093–5096 (1998).
10. Mai, M., Cheng, X. M., Li, X. G. & Zhang, P. Quantum dynamics of the molecular magnet driven by external magnetic fields. *Phys. Rev. B* **70**, 214408 (2004).
11. Russell, P. St. J. Photonic crystal fibers. *Science* **299**, 358–362 (2003).
12. Dudley, J. M., Genty, G. & Coen, S. Supercontinuum generation in photonic crystal fiber. *Rev. Mod. Phys.* **78**, 1135–1184 (2006).
13. Lenz, G., Talanina, I. & de Sterke, C. M. Bloch oscillations in an array of curved optical waveguides. *Phys. Rev. Lett.* **83**, 963–966 (1999).
14. Christodoulides, D. N., Lederer, F. & Silberberg, Y. Discretizing light behaviour in linear and nonlinear waveguide lattices. *Nature* **424**, 817–823 (2003).
15. de Sterke, C. M., Bright, J. N., Krug, P. A. & Hammon, T. E. Observation of an optical Wannier-Stark ladder. *Phys. Rev. E* **57**, 2365–2370 (1998).
16. Morandotti, R., Peschel, U., Aitchison, J. S., Eisenberg, H. S. & Silberberg, Y. Experimental observation of linear and nonlinear optical Bloch oscillations. *Phys. Rev. Lett.* **83**, 4756–4759 (1999).
17. Pertsch, T., Dannberg, P., Elflein, W., Brauer, A. & Lederer, F. Optical Bloch oscillations in temperature tuned waveguide arrays. *Phys. Rev. Lett.* **83**, 4752–4755 (1999).
18. Trompeter, H. *et al.* Bloch oscillations and Zener tunneling in two-dimensional photonic lattices. *Phys. Rev. Lett.* **96**, 053903 (2006).
19. Wan, J., Laforest, M., de Sterke, C. M. & Dignam, M. M. Optical filters based on dynamic localization in curved coupled optical waveguides. *Opt. Commun.* **247**, 353–365 (2005).
20. Iwanow, R. *et al.* Discrete Talbot effect in waveguide arrays. *Phys. Rev. Lett.* **95**, 053902 (2005).
21. Sukhorukov, A. A., Neshev, D. N. & Kivshar, Yu. S. Shaping and control of polychromatic light in nonlinear photonic lattices. *Opt. Express* **15**, 13058–13076 (2007).
22. Garanovich, I. L., Sukhorukov, A. A. & Kivshar, Yu. S. Broadband diffraction management and self-collimation of white light in photonic lattices. *Phys. Rev. E* **74**, 066609 (2006).
23. Garanovich, I. L. *et al.* Diffraction control in periodically curved two-dimensional waveguide arrays. *Opt. Express* **15**, 9737–9747 (2007).
24. Nolte, S., Will, M., Burghoff, J. & Tuennermann, A. Femtosecond waveguide writing: A new avenue to three-dimensional integrated optics. *Appl. Phys. A* **77**, 109–111 (2003).
25. Szameit, A. *et al.* Two-dimensional soliton in cubic fs laser written waveguide arrays in fused silica. *Opt. Express* **14**, 6055–6062 (2006).
26. Szameit, A. *et al.* Observation of two-dimensional surface solitons in asymmetric waveguide arrays. *Phys. Rev. Lett.* **98**, 173903 (2007).
27. Szameit, A. *et al.* Quasi-incoherent propagation in waveguide arrays. *Appl. Phys. Lett.* **90**, 241113 (2007).
28. Trompeter, H. *et al.* Visual observation of Zener tunneling. *Phys. Rev. Lett.* **96**, 023901 (2006).
29. Neshev, D. N. *et al.* Nonlinear spectral-spatial control and localization of supercontinuum radiation. *Phys. Rev. Lett.* **99**, 123901 (2007).
30. Sukhorukov, A. A. *et al.* Polychromatic nonlinear surface modes generated by supercontinuum light. *Opt. Express* **14**, 11265–11270 (2006).


## Acknowledgements

We thank M. de Sterke and B. Eggleton for useful discussions and comments. The work has been supported by the Australian Research Council through a Discovery Project and Centre of Excellence CUDOS, by the German Ministry of Education and Research (Research Unit 532) and by the Leibniz program of the Deutsche Physikalische Gesellschaft.

## Author contributions

The experimental work was carried out by A.S., M.H., F.D., T.P., S.N. and A.T. The theory was developed by I.L.G., A.A.S and Yu.S.K. The numerical modelling was carried out by I.L.G. and A.A.S.

## Additional information

Reprints and permissions information is available online at http://npg.nature.com/reprintsandpermissions. Correspondence and requests for materials should be addressed to A.S.